

INFLUENCE OF PLASTIC TENSION CHORD DEFORMATION ON THE SHEAR CAPACITY OF PRESTRESSED BEAM ELEMENTS

SEBASTIAN THOMA*, OLIVER FISCHER

Technical University of Munich, Chair of Concrete and Masonry Structures, Theresienstraße 90, N6, 80333 München, Germany

* corresponding author: sebastian.thoma@tum.de

ABSTRACT. The shear strength of prestressed beam elements is of great interest with regard to the evaluation of existing concrete bridges. Accompanying extensive experimental test series, the adaptation and modification of existing models for the evaluation of the load-bearing capacity also represents an important step. Against this background, considerations are made for the isolation of critical influencing factors on the effective concrete compressive strength and quantified on the basis of a numerical framework. Subsequently, a sensitivity analysis is performed on this basis to determine the influence of individual parameters and their interaction. Taking into account the non-linear relationships at the cross-section level and in the cracked compressive stress field in the web, the shear reinforcement ratio and the strain in the longitudinal reinforcement are of major importance.

KEYWORDS: Plastic tension chord, prestressed concrete, sensitivity analysis, shear strength, stress fields.

1. INTRODUCTION

For the assessment of existing bridge structures and with respect to special questions related to prestressed concrete bridges, theoretical and experimental efforts to evaluate the shear capacity have been increased in the recent past [1–3]. In particular, characteristic bearing mechanisms of prestressed continuous girders with a low amount of shear reinforcement are continuously under discussion. From own experimental investigations, which are briefly presented schematically in section 2, the question for the evaluation of possible influencing factors on the effective concrete compressive strength of the cracked compressive stress field is developed and described by means of a numerical model, cf. section 3. Subsequently, the proportion of the variance of the individual input variables in the total variance of the response spectrum is evaluated using a global sensitivity analysis [4] in section 4. From this, dominant parameters and model-inherent interactions can be derived. Section 5 discusses main results and some influences of the numerical model are evaluated. Existing approaches to consider the phenomenon of compression softening together with the presented results may be viewed from a new angle. This procedure provides a valuable basis for possible model modifications based on it.

2. EXPERIMENTAL EVIDENCE

The aim of the experimental research is the systematic illustration of the influence of a gradually reduced degree of longitudinal reinforcement and the associated effects on internal equilibrium. For this purpose, nine prestressed beam elements are tested using the substructure technique. Figure 1 illustrates the concept.

This method has already been deployed at the institute to study various aspects in regard to the shear strength of prestressed beam elements [1, 5], while the basic idea for testing detached subsystems has already been used successfully before [6]. Including digital image correlation and fibre-optic sensors along longitudinal reinforcement and tendon axis, the experimental results show that the force flow in prestressed beams is subject to a highly statically indeterminate interaction that adopts a static equilibrium depending on communicating damage processes. In this way, the shear capacity is not considered in an exposed manner, but is to be classified with conformity of the stresses and strains under all acting internal forces, whereby in particular the mixed reinforced tension chord of reinforcing steel and tendon controls the cross-sectional strain and dominance of individual load-bearing components.

The analysis shows that even with yielding longitudinal reinforcement under high bending moments in field and support regions, the ultimate system capacity is determined by a shear failure as long as the prestressing steel can provide the corresponding increase in strain. The evaluation of the tension chord deformation and the evolution of the cracked stress field in the web prove the great importance of arching actions in the description of the bearing behaviour of prestressed beam elements. A comprehensive analysis and discussion of experimental results will be presented in other publications and are not the subject of this paper. The brief outline of the experiments carried out is intended solely as a background and forms the basis for the considerations set out below, which can assist in evaluating the results and further refining the model concepts.

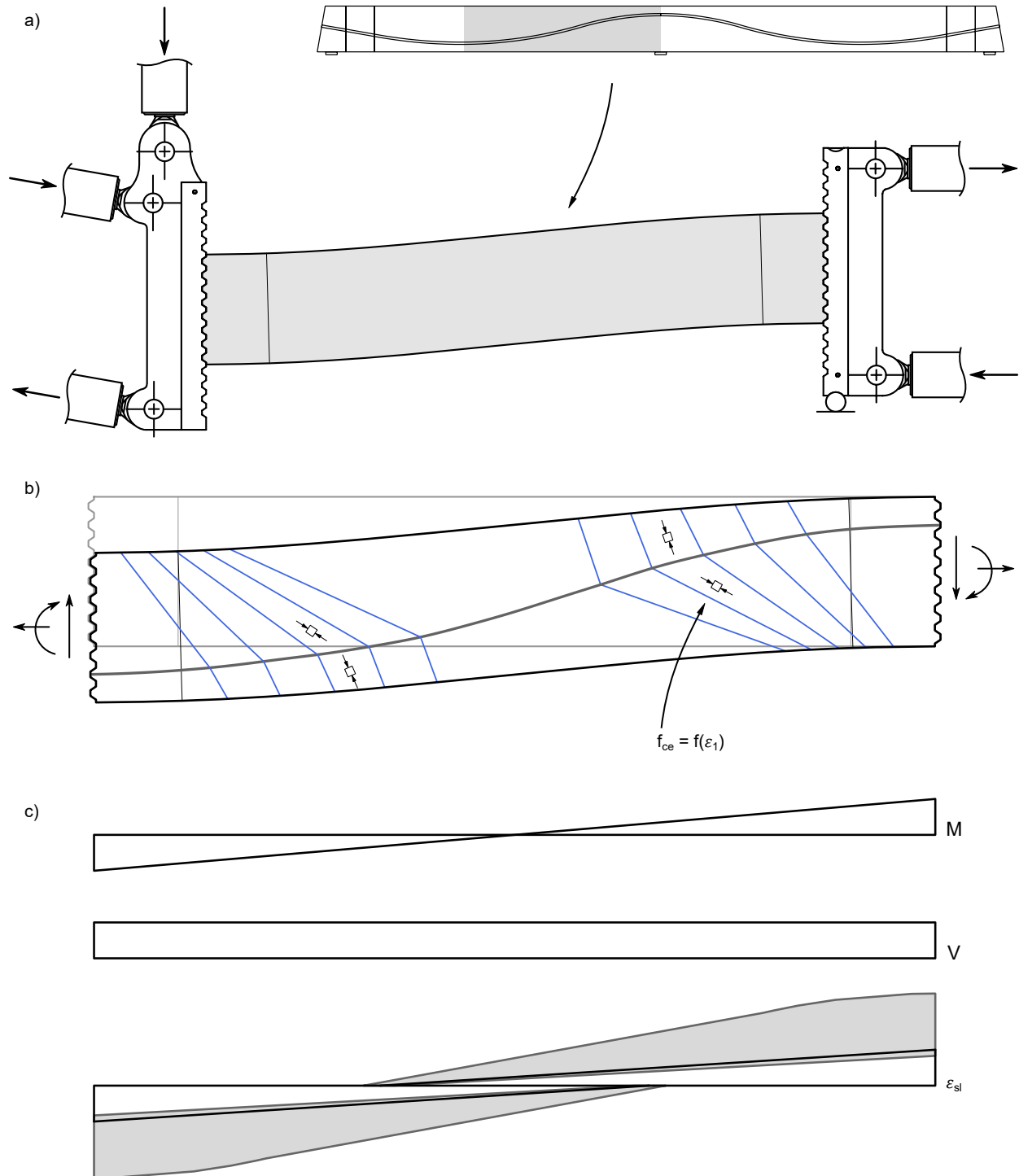


FIGURE 1. Experimental setup and focus of presented studies:

a) Substructure technique for investigating the shear strength of prestressed beam elements, based on the shear field of a continuous beam between the point load in the span and the inner support. Reinforcement and tendons are anchored in tension in the cut edges/load plates; b) Deformed system and internal forces acting on it. The push cam profiling enables the transmission of shear forces in analogy to bridges in segmental construction. The fans of the cracked compressive stress field are indicated in the field and support areas, a deflection takes place at tendon axis. The effective web compressive strength, controlled by the reduction factor k_c , is the focus of the presented investigations. Relevant details related to this factor are explained in the following section 3; c) Qualitative profile of bending moment and shear force in the tested beam element. The load is successively increased until a shear failure occurs. Under increasing load and a considerably reduced degree of longitudinal reinforcement, plastic strains result in the longitudinal reinforcement, which require a corresponding increase in strain in the tendons in order to guarantee the equilibrium of the internal forces.

3. COMPRESSION SOFTENING APPROACH

3.1. BACKGROUND

Taking into account the test results, which show that the system load-bearing behaviour of prestressed cross-sections is still limited by the shear capacity despite plastic tension chord deformation, and based on assumptions of the plasticity theory for the prediction of the shear strength, the effective concrete compressive strength of the cracked stress field is of crucial importance.

As stated in [7], the assumption of a shear force bearing capacity derived from shear reinforcement is always limited by the bearing capacity of the concrete compression struts, which in turn depends on the effective concrete compressive strength and thus on the general state of strain. As a result, in addition to the shear reinforcement ratio, the longitudinal reinforcement ratio and the longitudinal strain - coupled by the load distribution and system slenderness - may have a major influence on the shear force bearing capacity. The factor k_c , see equations 4 and 5, thus decides on the extent to which plasticity-theoretical approaches can be used to describe the shear strength of reinforced concrete beams.

For design purposes, the effective concrete compressive strength is usually determined using constant reduction factors, which is a simple, conservative estimate. In the course of one's own considerations, and especially in the case of plastic chord deformation, it is reasonable to explicitly take into account the actual state of strain. Concrete girders, and in particular prestressed systems, develop a varying strain over beam height. The development of arching actions and the deviation of the stress field at the tendon axis cannot be represented in panel tests, which have contributed significantly to the description of various compression softening approaches [8–10]. Still, the relations within the membrane element can be transferred to the beam web if an equivalent measure of the longitudinal distortion can be formulated. Following the convention in the fib Model Code 2010 [11] or respectively the Modified Compression Field Theory (MCFT) [9, 12], the measure of effective longitudinal strain is defined at the mid-depth of the member. However, the member is not defined by the cross-sectional contour, but must be understood as a web (following a classical plasticity-theoretical cross-sectional division) between compression and tension chord. The longitudinal strain at half the height of the inner lever arm of the chord forces may serve as a clearer formulation here.

3.2. NUMERICAL MODEL

For the weighted evaluation of dominant influencing factors on the reduction factor k_c and consequently on the effective concrete compressive strength, various assumptions are linked to a numerical model, the

solution of which is solved as an optimisation problem, using sequential least squares [13, 14]. By iterating the strain plane for a cross-section under an acting bending moment and normal force, the lever arm of the internal forces is given after integrating the concrete compressive stresses, cf. figure 2. At the level of $z_m/2$, the average longitudinal strain state is obtained, which is further supplemented by components caused by shear, cf. equation 1, adopted from [7].

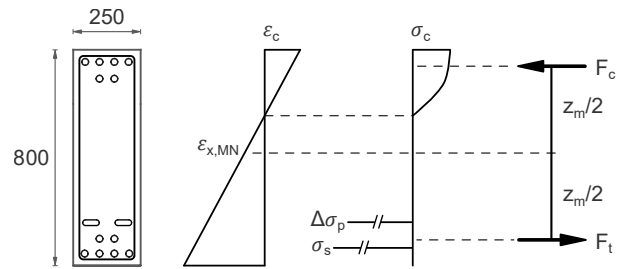


FIGURE 2. Investigated cross section [mm], strain, stress, inner forces and decisive strain $\epsilon_{x,MN}$ due to bending and axial forces

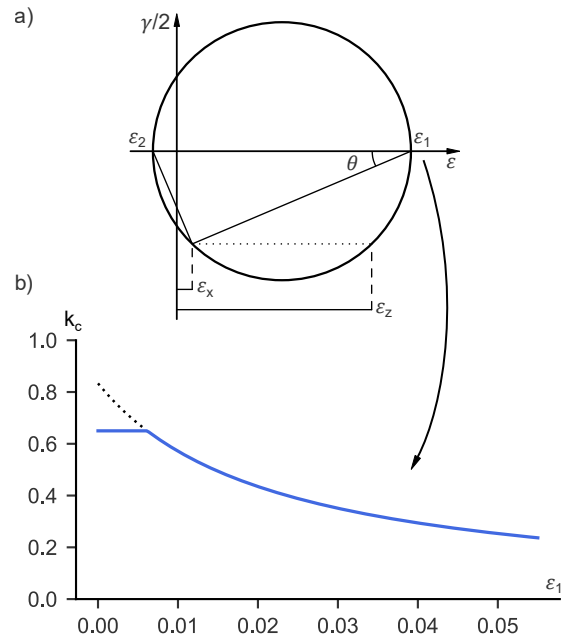


FIGURE 3. Core components of the optimisation problem: a) Mohr's circle of strains in pure shear b) Reduction factor k_c , introduced equation according to [10, 15]

Since the proportion of longitudinal strain due to shear $\epsilon_{x,V}$ is already formulated as a function of the compressive strut angle θ , equation 1 is already part of the constrained nonlinear optimisation. Based on equilibrium conditions and an explicit consideration

of the strains in longitudinal and shear reinforcement, which limit the range of possible strut angles (for a more detailed discussion, please refer to [7, 15]), the correlated values of the compression strut inclination and reduction factor k_c , respectively the effective compressive strength f_{ce} , can be determined, cf. equations 4 and 5. Assuming θ can evolve freely, taking into account its boundary conditions (derived from the yield strength and tensile strength of the reinforcement), the angle can be determined according to equation 2. The iterative routine is obvious in linking equation 2 and figure 3.

After convergence the further steps are straightforward, and the principal strain ε_1 as well as the reduction factor k_c are determined, cf. equations 3 and 4.

$$\varepsilon_{x,V} = \frac{V/2 \cdot \cot \theta}{2(z_s/z_m \cdot E_s A_s + z_p/z_m \cdot E_p A_p)} \quad (1)$$

$$\tan \theta = \sqrt{\frac{\rho_{sw} f_y}{f_{ce} - \rho_{sw} f_y}} \quad (2)$$

$$\varepsilon_1 = \varepsilon_{x,MNV} + (\varepsilon_{x,MNV} - \varepsilon_{c2}) \cdot \cot^2 \theta \quad (3)$$

$$k_c = \frac{1}{1.2 + 55 \cdot \varepsilon_1} \leq 0.65 \quad (4)$$

$$f_{ce} = k_c \cdot \left(\frac{30}{f_c}\right)^{1/3} \cdot f_c \quad (5)$$

The model uses additional, generally accepted simplifications, which are essentially due to the basic outlines of plasticity theory and will not be the focus of further attention here. Related to the proposed model structure, some questions with respect to model sensitivity arise:

- The principal strain ε_{c2} is assumed to be constant at -0.002. Is this, essentially empirically based, assumption [9] valid or do implicitly considered influencing factors falsify a generally valid statement?
- What are the consequences of an increased strain level in the longitudinal reinforcement for established models for predicting the shear strength in prestressed beam elements? Is ε_x a sensitive parameter for the response surface Y?
- Are there significant interaction effects between different input parameters of the model?

4. GLOBAL SENSITIVITY ANALYSIS

To address the above questions, the numerical model from section 3.2 is subjected to a sensitivity analysis. A global sensitivity analysis (GSA) distils the influence of possible uncertainty of selected n input parameters on the result of a model. Possible interactions of the input values (so-called second order effects) can also be determined by variance-based methods. In the

following *Sobol's Method* [16, 17] enables a quantified evaluation of these issues. Essential information on the characteristics of the GSA approaches used in this research is based on the considerations in [4], unless otherwise referenced. The method does not require an analytical model, but forms its correlation ratio on the basis of a problem spectrum to be defined initially, which contains all input parameters (which may be subject to the GSA), their distribution function and possible bounds. This data set is mapped into n dimensions by means of low-discrepancy sampling and then passed individually to the numerical model. Critical aspects and details of the implementation are described below.

4.1. SOBOL'S SEQUENCE

Aiming for minimized discrepancy, generated sequences of parameter values should avoid holes and clusters in the hypercube. This task is adequately accomplished by Sobol's sequences [16, 17]. In addition, Sobol's sequence ensures order independence for different input parameter axes. Without going into further detail, this is enabled by its direction numbers which are derived from distinct primitive polynomials for every required parameter vector [18]. Sobol' sequences are a quadrature rule and become unstable if samples of a size that is not a power of 2 are used, or if the first point is omitted, or if a sequence becomes sparse [19]. This method thus offers a tried and tested approach for evenly covering possible parameter constellations, which essentially eliminates the danger of unfavourable density of a parameter constellation. Figure 4 shows an example of uniformly distributed random coordinates and the spread using a Sobol' sequence. The difference in the uniform coverage of the area is obvious.

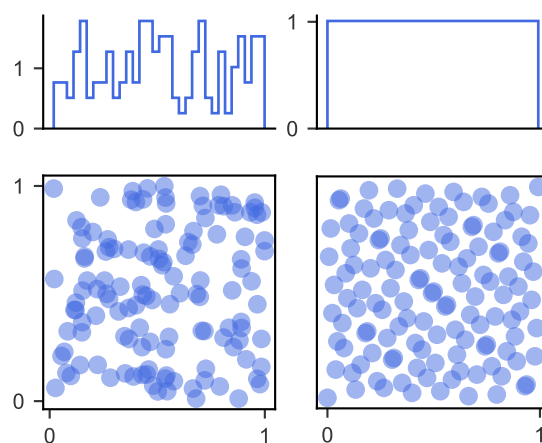


FIGURE 4. Random samples and Sobol' sequence in two dimensions ($2^7 = 128$ samples)

The model study accounts for seven parameters, which are listed in table 1 together with their assumed

uniform distribution. Uniform distributions are assumed for the parameter space because no specific configuration with known uncertainty is to be examined, but an overall impression and overview of the model sensitivity is to be given. The limit values of the distributions are based on the test programme referred to at the beginning or assumed as realistic limit values when considering existing reinforced concrete bridges. All parameters are part of the resistance side and are included in the iteration of the initial strain plane and/or subsequent iteration to determine the stress and strain state in the web. In addition to the range of the longitudinal reinforcement ratio, the lower limit of which leads to plastic chord deformations in the cross-section analysis, the shear reinforcement ratio is also chosen relatively low with regard to the conditions in existing prestressed concrete bridges. Taking into account the applied variation of the concrete compressive strength, a bandwidth of about 0.7 to 4.0 times the minimum shear reinforcement ratio $\rho_{w,\min}$ results for the general case according to $\rho_{w,\min} = 0.16f_{ctm}/f_{yk}$ [20].

Only λ represents a component of the load side to a certain extent, since the ratio of acting moment, which is increased independently of the GSA for all combinations of possible input values, and shear force, which also has a share in ε_x (see equation 1), is controlled via a variation of the shear slenderness. In addition, the variation of the tendon slope influences the effective shear force (after subtracting the vertical component $V_p = P_{mt} \cdot \sin \alpha_p$) in the web and ultimately the proportion $\varepsilon_{x,v}$.

Parameter	Uniform distr.	range
ρ_{sl}	[%]	[0.8, 2.0]
ρ_{sw}	[%]	[0.09, 0.36]
λ	[-]	[2.5 - 5.0]
ε_{c2}	[-]	[-0.002, -0.001]
f_c	[MPa]	[30.0, 50.0]
σ_p	[MPa]	[550.0, 600.0]
α_p	[deg]	[1.0, 7.0]

TABLE 1. Input parameters for sensitivity analysis.

Variance-based methods are powerful in quantifying the relative importance of input factors or groups. The main drawback of variance-based methods is the cost of the analysis, which, in the case of computationally intensive models, can become prohibitive even when using the approach described above. With Saltellis extension of the Sobol's sequence [17], which is used within this scope, the resulting matrix has $N(2n + 2)$ rows, where n is the number of parameters. For a full set of Sobol' indices (S1, S2 & ST, cf. section 4.2) a model with 7 factors requires to execute the model at least 16000 times, taking $N = 1000$. Whether the assumption for N was chosen sufficiently large can be judged from the confidence intervals. This results in over 200.000 model evaluations in total due to a

relatively finely chosen incremental bending moment rise.

In a general case, the validity and robustness of a composite indicator, in this case the reduction factor k_c may depend on a number of factors.

- The model chosen for estimating the measurement error in the data
- The mechanism for including or excluding indicators in the index; The choice of factors fed into a GSA is subjective. Particularly in the case of comparatively complex, non-linear numerical models, the model character itself has a considerable influence on the response surface Y . Theoretically, one could provide the GSA with as many input parameters as possible, but this seems unnecessarily CPU-intensive. Not pursued further here, but possible in the first place, seems to be the gradual reduction of the input parameters with subsequent evaluation of the correlation coefficient to the results of a fully packed analysis without static default values. Alternatively, qualitative screening using the Morris method [21] can be performed as the first step in model survey.
- The indicators preliminary treatment; In the investigations presented here, the limiting value 0.65 according to equation 4 is used in the framework of the iteration. The GSA evaluation deliberately excludes this criterion in order to take into account possible influences caused by the asymptotic character of the equation at low principal tensile strains.
- The type of normalization scheme applied to the indicators to remove scale effects
- The amount of missing data and the imputation algorithm; Under high bending moment, it is theoretically possible that the iteration of the strain plane does not reach a stable equilibrium according to the defined stress-strain relationships and limit strains. This leads to a lack of the input value $\varepsilon_{x,MN}$ in the further iterative consideration of the conditions for the web element, and to a non-response bias depending on the error handling. This scenario was prevented by previous comparative calculations so to avoid inconvergent result data falsifying the GSA.

4.2. SOBOL'S METHOD

After running the numerical model for Sobol's sequence, one gets an array that forms the so-called response surface. Sobol's method evaluates the part of the total variance of the response that can be attributed to input parameter X_n . The numerical implementation is based on the SALib package [22]. Three measures can be obtained for each parameter:

- first order index S1: contribution (without interaction) of a parameter to the response variance
- second order index S2: interaction of input parameters to the response variance

- total effect index ST: total contribution (including interaction) of a parameter to the response variance

A measure of sensitivity is to calculate the variance of the conditional expectation $Var[E(Y|X_n)]$ referred to the total variance of Y, $Var(Y)$, cf. equation 6. In other words, the total variance of the response Y that can be attributed to input parameter X_n defines its weight within the numerical model and, in a further step, enables a better understanding of model-inherent features beyond qualitative screening and, ultimately, opens up initial starting points if a model modification appears desirable.

$$S1_n = \frac{Var[E(Y|X_n = x_n)]}{Var(Y)} \quad (6)$$

Any numerical model is some sort of mapping input parameters to output results. The following equation 7 shows the added parts that influence the result y, namely scalar values, the sum of functions evaluated for each parameter (modelling the effect of each individual parameter) and the interaction of parameters.

$$\begin{aligned} y = f(x) = & f_0 \\ & + \sum_{n=1}^{N_p} f_n(x_n) \\ & + \sum_{1 \leq n' \leq N_p} f_{n,n'}(x_n, x_{n'}) \\ & + \dots + f_{1,2,\dots,N_p}(x_1, \dots, x_{N_p}) \end{aligned} \quad (7)$$

The total variance of the response Y (the total of all y-evaluations) can be decomposed into partial variances, attributing variability of the response Y to each input parameter, including interactions. Different conditional variances:

$$D_n = Var[E(Y|X_n)] \quad (8)$$

Variance on two conditions:

$$D_{n,n'} = Var[E(Y|X_n, X_{n'})] - D_n - D_{n'} \quad (9)$$

The first order Sobol' index $S1_n$ calculates the impact of the input parameter X_n by estimating the partial variance of Y explained by this parameter. It estimates by how much the variance of the response is reduced, on average, when the parameter X_n is fixed, i.e. it measures the contribution of the parameter X_n to the total variance of the response. The total effect index for a parameter X_n is defined:

$$ST_n = S_n + \sum_{n \leq n'} S_{n,n'} + \dots \quad (10)$$

The total effect index represents the total contribution (including interactions) of a parameter X_n to the response variance; it is obtained by summing all first-order and higher-order effects involving the parameter X_n . Further input variables of the model

that are not included in the GSA, but are nevertheless to explicitly assume a variable character, require a recalculation of the sensitivity indices for all Sobol' samples. In the present case, this is the case for the applied bending moment from external load. This procedure is comparatively computationally intensive, but it allows a view on a potentially variable prioritisation of the parameters according to Table 1, which should be quite common, especially for non-linear model considerations.

5. RESULTS AND DISCUSSION

The GSA shows which of the selected input parameters have an influence on k_c and which values would have been sufficiently taken into account within the scope of the investigations with the assumption of a constant value, since no significant contribution to the variance of the result is evident. The major factor is the transverse reinforcement ratio. It is the most important influencing variable over the complete variation of the moment acting on the cross-section. This seems to be plausible with regard to equation 2. Described from a phenomenological point of view, the stirrup strain imposes a proportional transverse strain on the concrete compression struts, which reduces the effective concrete compressive strength. For low shear reinforcement levels, this issue is particularly critical because the small cross-sectional area mobilises high strains early on for comparatively small forces after shear cracking. Depending on the crack opening and ductility of the reinforcement, rupture of the reinforcement may occur. Further questions arise in this regard, which will not be discussed in detail here.

A model without parameter interaction leads to $\sum ST = 1$, which is obviously not the case here. Under external bending moment of about 0.45 to 0.5 MNm, interesting dependencies between longitudinal and shear reinforcement ratio are revealed, cf. figure 5. The concrete compressive strength also appears to gain in importance in the meantime before ST settles back down to the initial level. Figure 6 shows also a remarkable interaction between ρ_{sw} and ε_{c2} develop in this range. This intermediate effect is due to the limiting conditions of the possible bandwidth of permitted compression strut angles. After exceeding the decompression stresses, small longitudinal strains of the same order of magnitude as ε_{c2} initially enter into the equations. As expected, the influence of the longitudinal strain rises under increasing moment, while the shear reinforcement ratio, which is still important, decreases significantly. A moment of 0.9 MNm for the considered example cross-section (figure 2) results in the longitudinal reinforcement reaching its yield stress.

The high longitudinal strain $\varepsilon_{x,MNV}$ becomes more important for the iterative determination of the compression strut angle and the principal strain ε_1 under increasing load. Against the background of high utilization rates for bending and shear of many existing

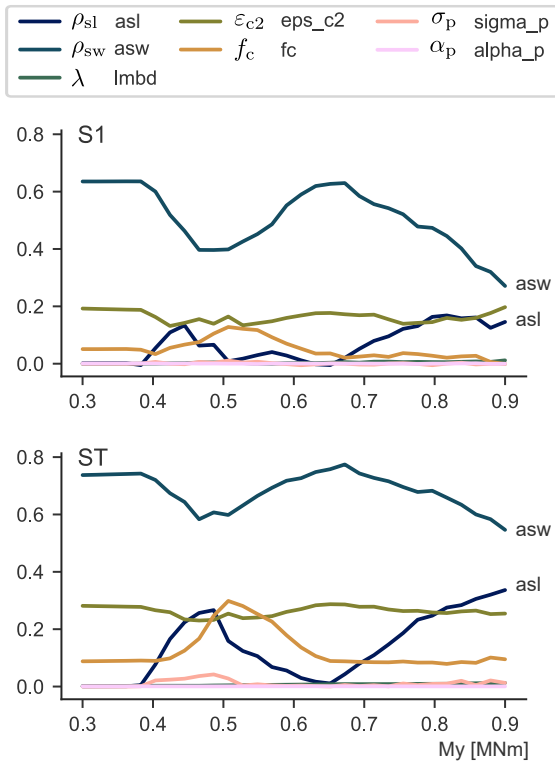


FIGURE 5. Individual parameter importance S1 and total prioritisation ST affecting k_c

concrete bridges, the question arises to what extent the mostly constant factors in standards provided represent a reasonable assumption. Directly linked to this is, of course, the question of an adequate formulation of the effective concrete compressive strength or, at a distance, the question of the fundamental capacity of the model conception for shear strength discussed here. The generally constant assumption of the principal strain ϵ_{c2} even proves to be a definite parameter to be taken into account, largely independent of the acting moment, if one considers modifying the numerical model with respect to k_c . The importance of a reasonable assumption or parameterized formulation for ϵ_{c2} becomes clear when looking at figure 3. Selected principal compressive strain and longitudinal strain ϵ_x are of the same order of magnitude in absolute terms and have an influence on the compression strut angle according to their difference.

6. CONCLUSIONS

The paper presents a numerical model that allows a closed-loop determination of the effective concrete compressive strength in a beam web under shear loading. Of further interest is the reduction factor k_c used, which is influenced to different degrees by different parameters. In order to determine the individual influence of the parameters and possible model-determined interaction effects, a GSA was carried out, which was able to identify the shear reinforcement ratio and the assumption of the principal strain ϵ_{c2} in general, and

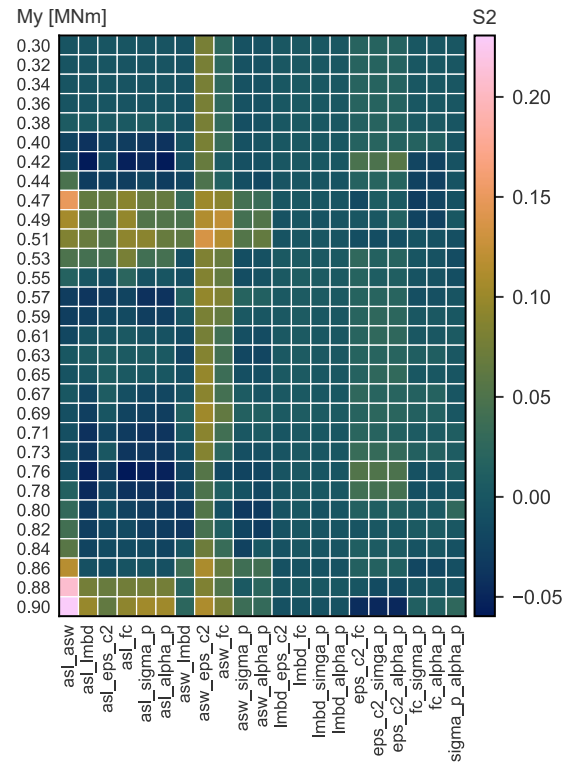


FIGURE 6. S2 Indices: Input Parameter interaction affecting k_c

the longitudinal reinforcement ratio and corresponding, ultimately plastic chord deformation under high moment loading in particular as the decisive adjusting screws.

In light of the experimental investigations, which achieved high shear capacities despite plastic chord deformation, a few questions arise:

- Do the empirically derived formulations for determining the reduction factor k_c sufficiently approximate the conditions in a prestressed beam web or are the model ideas of plasticity theory described here (especially for cross-sectional segmentation) not applicable?
- Which possibilities for a more refined estimation of the main strain ϵ_{c2} seem practicable and reasonable?

These questions are part of further considerations, which should be evaluated in the context of the ductility of the reinforcement, which was already briefly addressed in the course of the discussion of results.

LIST OF SYMBOLS

- k_c Reduction factor for concrete compressive strength due to transverse tensile strain [-]
- ϵ_c Concrete strain [-]
- $\epsilon_{x,MN}$ Axial concrete strain due to normal forces and bending moment at half the height of the inner lever arm [-]
- $\epsilon_{x,V}$ Axial concrete strain due to shear [-]
- ϵ_1 Concrete principal tensile strain [-]

ε_2 Concrete principal compressive strain [-]
 θ Compression strut angle [deg]
 f_{ce} Effective concrete compressive strength [MPa]
 f_c Concrete compressive strength, derived from cylinder tests [MPa]
 ρ_{sl} Longitudinal reinforcement ratio, defined as $\rho_{sl} = A_{sl}/(b_w \cdot d)$ [-]
 ρ_{sw} Geometric shear reinforcement ratio, defined as $\rho_{sw} = a_{sw}/b_w$ [-]
 λ Shear slenderness, defines as $\lambda = M/(V \cdot d)$ [-]
 z_m Lever arm of inner forces [mm]
 z_s Lever arm between F_c and F_s [mm]
 z_p Lever arm between F_c and F_p [mm]
 σ_c Concrete (compressive) stress [MPa]
 σ_s Steel stress due to normal forces and bending moment [MPa]
 σ_p Prestress in tendons [MPa]
 $\Delta\sigma_p$ Increased tendon stress due to normal forces and bending moment [MPa]
 α_p Tendon slope [deg]
 F_c Resultant inner compressive force [MN]
 F_t Resultant inner tension force as weighted sum of F_s and F_p [MN]
 V Shear force [MN]
 E_s Modulus of elasticity of longitudinal reinforcement [MPa]
 E_p Modulus of elasticity of prestress tendon strands [MPa]
 A_s Cross-sectional area of longitudinal reinforcement in tension [m²]
 A_p Cross-sectional area of prestressed tendons [m²]
 $S1$ Sobol's first order index - individual parameter contribution to total response variance [-]
 $S2$ Sobol's second order index - contribution of parameter interactions (higher-order effects) to total response variance [-]
 ST Sobol's total index combines margins of $S1$ and $S2$ for each parameter [-]

REFERENCES

- [1] N. Schramm, O. Fischer. Zur Anrechenbarkeit von nicht normgemäßen Bügelformen auf die Querkrafttragfähigkeit von Bestandsbrücken. *Bauingenieur* **95**(11):408–418, 2020. <https://doi.org/10.37544/0005-6650-2020-11-66>.
- [2] P. Huber, T. Huber, J. Kollegger. Experimental and theoretical study on the shear behavior of single- and multi-span T- and I-shaped post-tensioned beams. *Structural Concrete* **21**(1):393–408, 2020. <https://doi.org/10.1002/suco.201900085>.
- [3] V. Adam, M. Herbrand, J. Hegger. Querkrafttragfähigkeit von Brückenträgern aus Spannbeton mit geringen Querkraftbewehrungsgraden. *Bauingenieur* **95**(11):397–407, 2020. <https://doi.org/10.37544/0005-6650-2020-11-55>.
- [4] A. Saltelli, M. Ratto, T. Andres, et al. *Global Sensitivity Analysis. The Primer*. 2007. <https://doi.org/10.1002/9780470725184>.
- [5] N. Schramm, O. Fischer. Querkraftversuche an profilierten Spannbetonträgern aus UHPFRC. *Beton- und Stahlbetonbau* **114**(9):641–652, 2019. <https://doi.org/10.1002/best.201900022>.
- [6] W. Kaufmann, P. Marti. *Versuche an Stahlbetonträgern unter Normal- und Querkraft*, vol. 226. Birkhäuser, Basel, Switzerland, 1996. <https://doi.org/10.3929/ethz-a-001734903>.
- [7] B. Hackbarth. *Zur Querkrafttragfähigkeit von Stahl- und Spannbetonträgern mit Bügelbewehrung*. Ph.D. thesis, TUHH, Hamburg, Germany, 2015.
- [8] A. Belarbi, T. T. C. Hsu. Constitutive Laws of Softened Concrete in Biaxial Tension Compression. *Structural Journal* **92**(5):562–573, 1995. <https://doi.org/10.14359/907>.
- [9] F. J. Vecchio, M. P. Collins. The Modified Compression-Field Theory for Reinforced. *Journal Proceedings* **83**(2):219–231, 1986. <https://doi.org/10.14359/10416>.
- [10] W. Kaufmann. *Strength and deformations of structural concrete subjected to in-plane shear and normal forces*. Ph.D. thesis, ETH, Zürich, Switzerland, 1998. <https://doi.org/10.3929/ethz-a-001945805>.
- [11] CEB. Model code 2010: First complete draft. Tech. rep., International Federation for Structural Concrete, Lausanne, Switzerland, 2010. <https://doi.org/10.35789/fib.BULL.0055>.
- [12] E. C. Bentz, F. J. Vecchio, M. P. Collins. Simplified Modified Compression Field Theory for Calculating Shear Strength of Reinforced Concrete Elements. *Structural Journal* **103**(4):614–624, 2006. <https://doi.org/10.14359/16438>.
- [13] D. Kraft. *A software package for sequential quadratic programming*. Wiss. Berichtswesen d. DFVLR, 1988.
- [14] P. Virtanen, R. Gommers, T. E. Oliphant, et al. SciPy 1.0: Fundamental Algorithms for Scientific Computing in Python. *Nature Methods* **17**:261–272, 2020. <https://doi.org/10.1038/s41592-019-0686-2>.
- [15] V. Sigrist. Generalized Stress Field Approach for Analysis of Beams in Shear. *Structural Journal* **108**(4):479–487, 2011. <https://doi.org/10.14359/51682989>.
- [16] I. M. Sobol'. Global sensitivity indices for nonlinear mathematical models and their Monte Carlo estimates. *Mathematics and Computers in Simulation* **55**(1):271–280, 2001. [https://doi.org/10.1016/S0378-4754\(00\)00270-6](https://doi.org/10.1016/S0378-4754(00)00270-6).
- [17] A. Saltelli. Making best use of model evaluations to compute sensitivity indices. *Computer Physics Communications* **145**(2):280–297, 2002. [https://doi.org/10.1016/S0010-4655\(02\)00280-1](https://doi.org/10.1016/S0010-4655(02)00280-1).
- [18] P. Jäckel. *Monte Carlo Methods in Finance*. Wiley, Hoboken, NJ, USA, 2002.
- [19] A. B. Owen. On dropping the first Sobol' point. *ArXiv e-prints* 2020. 2008.08051.
- [20] CEN. Eurocode 2: Design of concrete structures - part 2: Concrete bridges - design and detailing rules. Tech. rep., European Committee for Standardization, 2010.

[21] M. Morris. Factorial Sampling Plans for Preliminary Computational Experiments. *Technometrics* **33**(2):161–174, 1991.
<https://doi.org/10.1080/00401706.1991.10484804>.

[22] J. Herman, W. Usher. SALib: An open-source python library for sensitivity analysis. *The Journal of Open Source Software* **2**(9), 2017.
<https://doi.org/10.21105/joss.00097>.